

VERTICAL COUPLING IMPEDANCE OF THE APS STORAGE RING*

Yong-Chul Chae[†], Katherine Harkay, Xiang Sun

Advanced Photon Source, Argonne National Laboratory, Argonne, IL 60439 USA

Abstract

The three-dimensional wake potentials of the APS storage ring have been reconstructed according to the impedance database concept. Every wakefield-generating component in the ring was considered including small-gap insertion device (ID) chambers, rf cavities, shielded bellows, beam position monitors, synchrotron radiation absorbers, scrapers, flags, various chamber transitions, septum chambers, and pulsed kickers. In this paper the result for the vertical wake potentials and its impedance are presented. Dominant contributors are the ID chambers whose heights are 5 mm and 8 mm. Since more small-gap chambers are envisioned for installation in the APS storage ring, prediction of their effect on the beam is very important not only for the APS but also for all third-generation light sources. We used the vertical impedance reported here to investigate the measured tune slope and single-bunch current limit in the APS storage ring. The program *elegant* was used for particle tracking, and its results are presented. We also report that we observed a vertical focusing in the calculated wake potential of the shallow transition without rotational symmetry.

IMPEDANCE DATABASE

The concept of an impedance database is described in the companion paper [1]. We report highlights of building the database for the vertical impedance. The horizontal and longitudinal impedance are reported separately [2,3].

Insertion Device

The small gap chambers for insertion devices have been identified as having the most significant effect on the single-bunch current limit [4]. Therefore, the investigation of ID chamber effects is important and requires an accurate estimate of the impedance. Only the geometric impedance is considered in the impedance database; the resistive impedance is computed from analytical expressions and is not included.

Since the impedance calculation was performed using numerical simulation (we used the program MAFIA), the mesh size is one of the important parameters to be determined. For the bunch length of 5 mm we could use a 1-mm mesh. However, we found that we need a finer mesh of 0.5 mm in order to avoid numerical instability. A total of 17 million mesh points was required.

The impedance of ID chambers with 5-mm and 8-mm gaps are shown in Fig. 1. In the simulation we used two boundary conditions at the symmetry plane; one is that the electric field is equal to zero (E-wake) and the other is that the magnetic field is equal to zero (H-wake). The

total wake is $(E\text{-wake} + H\text{-wake})/2$. The Fourier transform of the total wake divided by the bunch spectrum is the impedance shown in Fig. 1. Among the two boundary conditions, E-wake dominates and is always positive (defocusing). However, the H-wake is small and could be negative (focusing).

The magnitude of the impedance for the different gap sizes, b , shows a b^{-3} dependence similar to resistive-wall impedance.

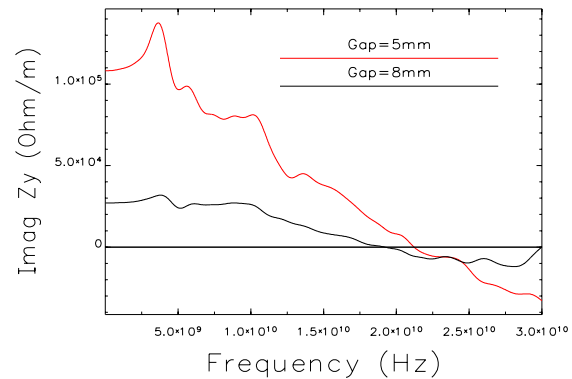


Figure 1: Impedance of ID chamber.

We knew that it was difficult to verify the accuracy of the numerical calculation of wake potentials for a 3-D transition because no reference exists with which to compare it. In order to increase our confidence in the 3-D calculation, we adopted a 2-D calculation as the reference that could be benchmarked later.

We constructed transitions for a circular chamber whose dimensions are comparable to the ID chamber; the geometry is shown in Fig. 2. We used two different programs, ABCI and MAFIA, to calculate the wake potential for the same geometry. The results from the two programs are compared in Fig. 3; it shows good agreement. Since the results from the 2-D program (ABCI) were highly accurate, we considered the results by MAFIA's simulations to be as accurate and reliable. This gave us confidence in the results presented in Fig. 1.

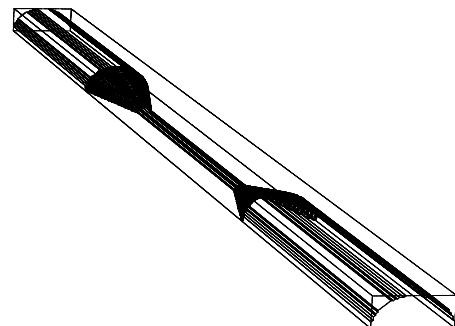


Figure 2: Circular transition.

* Work supported by the U.S. Department of Energy, Office of Basic Energy Sciences under Contract No. W-31-109-ENG-38.

[†] chae@aps.anl.gov

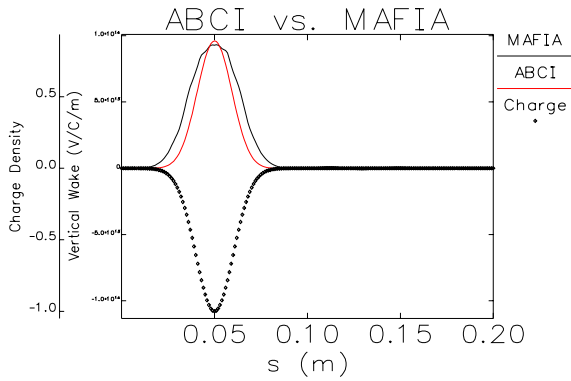


Figure 3: Vertical wake potentials by ABCI and MAFIA.

Synchrotron Radiation Absorber

In the APS storage ring, there are five synchrotron radiation absorbers per sector totaling 200 installed in the ring. They are all similar and one of them is shown in [3]. Since the absorber material intrudes on the horizontal side of the chamber without altering the vertical chamber dimension significantly, we expected a negative wake in the vertical plane if the empirical rule conjecture in [3] is true.

The MAFIA simulation resulted in a negative wake as shown in Fig. 4. Since the vertical beta function at the absorber location is high, the focusing effect of the negative wake is beneficial to the APS storage ring.

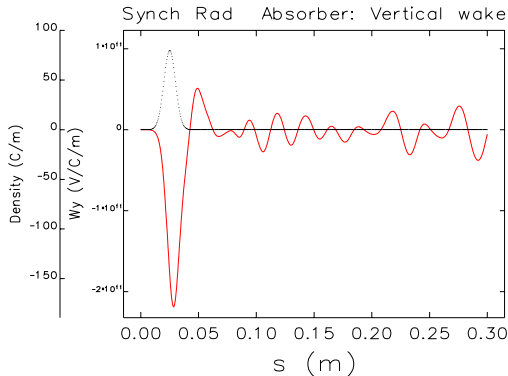


Figure 4: Vertical wake potential of absorber showing negative wake.

Other Components

Among the many components in the ring, one of the surprise was the flag chamber, of which there are ten in the ring. It has an rf screen in the chamber that forms a cavity-like structure; this contributes more than the anticipated impedance to the total. In addition, the mini-BPMs installed at the ID chamber also showed a negative wake potential, which was totally unexpected.

TOTAL IMPEDANCE

The total wake potential for a 5-mm bunch and the corresponding impedance are shown in Fig. 5. The shape of the wake is nearly proportional to the charge distribution. The impedance at low frequency is about 1.2 MΩ/m. A broad band resonator (BBR) was used to fit the imped-

ance; its parameters were found to be shunt impedance $R_s=0.5 \text{ M}\Omega$, quality factor $Q=0.4$, and resonant frequency $f_r=20 \text{ GHz}$.

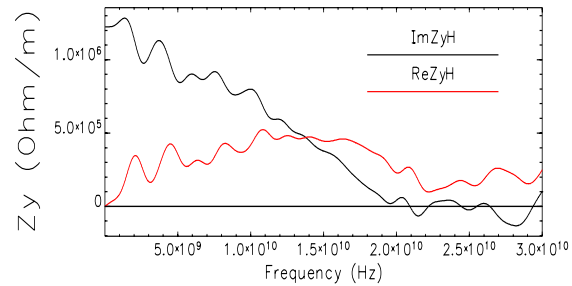
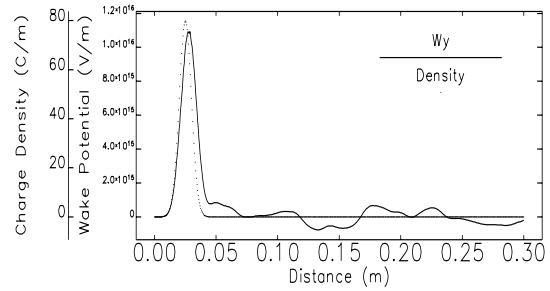


Figure 5: Total wake potential of the APS storage ring (top); the impedance (bottom).

The breakdown of the total impedance is presented in Fig. 6, which clearly shows that the dominant contributions are from 22 ID chambers of 8-mm gap together with 2 ID chambers of 5-mm gap.

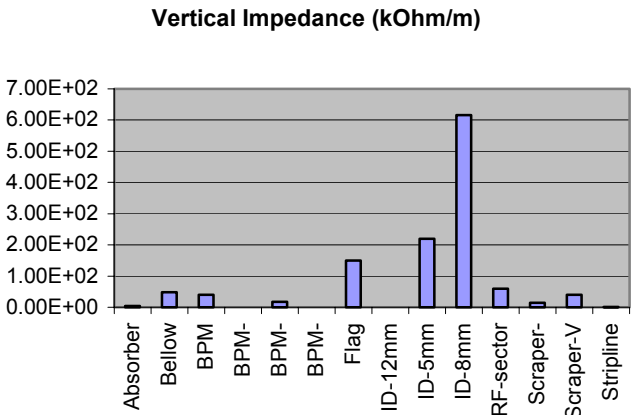


Figure 6: Breakdown of vertical impedance of the ring.

APPLICATION

We applied the total impedance to the APS storage ring in order to explain the various beam behaviors observed in the ring. A few examples are presented.

Tune Slope

Recently, the response matrix fit method [5] was used to measure the tune slope; the measured value was

$2.4 \times 10^{-3}/\text{mA}$, which was obtained by fitting the data in the range of current from 2 mA to 10 mA.

In order to estimate the tune slope by utilizing the total calculated impedance, we used the tune slope formula:

$$\frac{dv}{dI} = \frac{R}{2\pi\sigma_s E/e} \sum_{Elements} \beta Z_{eff},$$

where β_i is the betatron function at the location of the impedance element. The recently measured bunch length data were incorporated in the calculation, using the 2.5-nm lattice. The tune slope as a function of current is shown in Fig. 7. It shows that the resistive-wall contribution is much smaller than the geometric impedance. The average tune slope over a range of currents is found to be $2.6 \times 10^{-3}/\text{mA}$. This is in good agreement with the measured data.

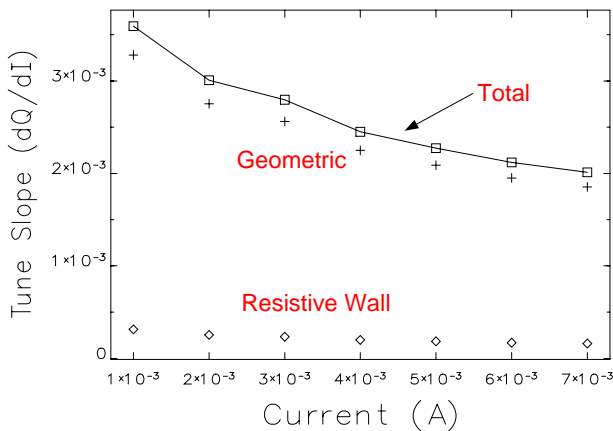


Figure 7: Tune slope as function of stored current in the 2.5-nm lattice with vertical chromaticity at 7.

Tracking Study

To understand the single-bunch current limit, we investigated the beam dynamics in the vertical plane by tracking multiple particles. We used the program *elegant* [6] to model a fully nonlinear lattice; the total impedance element is included at the location of the ID chamber.

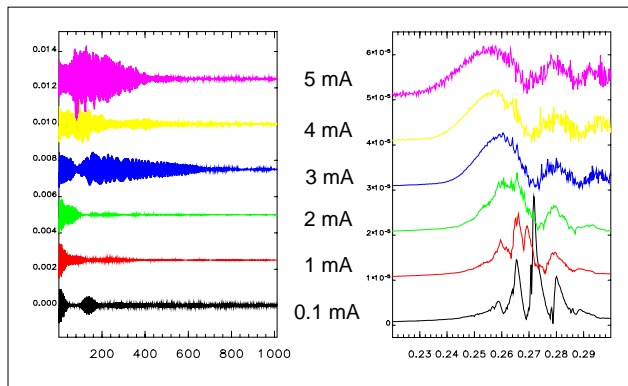


Figure 8: Turn-by-turn history of beam center (left); its Fourier transform (right).

In the simulation we kicked the beam once in the vertical plane and then recorded turn-by-turn histories of a number of beam parameters. One is the beam centroid as

shown in Fig. 8; several traces of various currents are depicted in a single graph. Also shown is the corresponding power spectrum, which reveals mode-coupling at 3 mA. We can see the effect of chromaticity modulation in the trace of low current of 0.1 mA. Above the mode-coupling threshold current of 3 mA the beam centroid is excited but subsequently damped fast. The amplitude of motion is not large enough to cause the particle loss

However, the history of the modeled beam size in Fig. 9 shows the significant blowup above the mode coupling. Since the dynamic aperture of the lattice is less than 10 mm, this blowup could cause the particle loss at 5 mA. The loss of particles was recorded in the simulation at the current 5 mA; the loss rate increased as the current increased. This may explain the observed limit of 8-10 mA in accumulating the current in a single bunch in the ring.

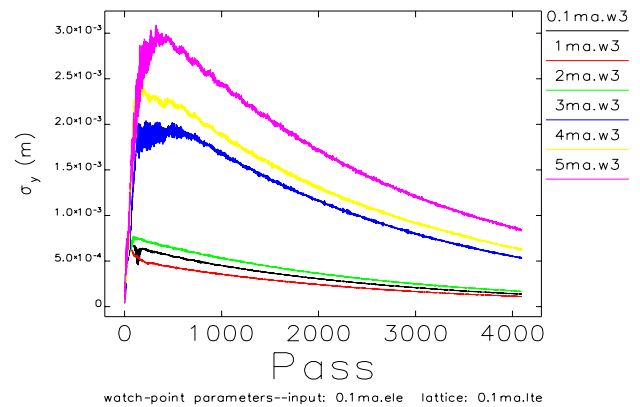


Figure 9: Turn-by-turn history of beam size showing blowup above the mode-merging current of 3 mA.

CONCLUSION

The impedance database concept was utilized to construct the total impedance of the ring. Modeling the APS ring using this impedance characterized well some of the observed beam behavior. The dominance of the small-gap chamber for ID has prompted research in reducing the vertical impedance through a new design of the chamber transitions.

REFERENCES

- [1] Y.-C. Chae, "The impedance database and its application to the APS storage ring," these proceedings.
- [2] Y.-C. Chae et al., "Horizontal coupling impedance of the APS storage ring," these proceedings.
- [3] Y.-C. Chae et al., "Longitudinal coupling impedance of the APS storage ring," these proceedings.
- [4] K.H. Harkay et al., Proc. 1999 PAC, 1644 (1999).
- [5] V. Sajaev, "Transverse impedance distribution measurements using the response matrix fit method at APS," these proceedings.
- [6] M. Borland, "elegant: A flexible SDDS-compliant for accelerator simulation," Advanced Photon Source Light Source Note 287, 2000.